NASA TECHNICAL NOTE

NASA TN D-7350

NASA TN D-7350

MOTION SOFTWARE FOR A SYNERGISTIC SIX-DEGREE-OF-FREEDOM MOTION BASE

by Russell V. Parrish, James E. Dieudonne, and Dennis J. Martin, Jr.

Langley Research Center
Hampton, Va. 23665

NATIONAL AERONAUTICS AND SPACE ADMINISTRATION • WASHINGTON, D. C. • DECEMBER 1973

1. Report No.	2. Government Accession No.	3. Recipient's Catalog No.
NASA TN D-7350		

4. Title and Subtitle	5. Report Date
MOTION SOFTWARE FOR A SYNERGISTIC SIX-DEGREE-OF-FREEDOM MOTION BASE	December 1973
	6. Performing Organization Code
7. Author(s)	8. Performing Organization Report No.
Russell V. Parrish, James E. Dieudonne, and Dennis J. Martin, Jr.	L-8798
	10. Work Unit No. 501-39-11-02
9. Performing Organization Name and Address	11. Contract or Grant No.
NASA Langley Research Center Hampton, Va. 23665	
	13. Type of Report and Period Covered
12. Sponsoring Agency Name and Address	Technical Note
National Aeronautics and Space Administration Washington, D.C. 20546	14. Sponsoring Agency Code

15. Supplementary Notes

Dennis J. Martin, Jr., is an employee of Electronic Associates, Inc.

16. Abstract

Computer software for the conversion of fixed-base simulations into moving-base simulations utilizing a synergistic six-degree-of-freedom motion simulator has been developed. This software includes an actuator extension transformation, inverse actuator extension transformation, a centroid transformation, and a washout circuit. Particular emphasis is placed upon the washout circuitry as adapted to fit the synergistic motion simulator. The description of the washout circuitry and illustration by means of a sample flight emphasize that translational cue representation may be of good fidelity, but care in the selection of parameters is very necessary, particularly in regard to anomalous rotational cues.

17. Key Words (Suggested by Author(s))	18. Distribution Statement
Synergistic motion base Washout system Coordinated washout Motion base software	Unclassified – Unlimited

19. Security Classif. (of this report)	20. Security Classif. (of this page)	21. No. of Pages	22. Price*
Unclassified	Unclassified	43	Domestic, $3.00 Foreign, $5.50

*For sale by the National Technical Information Service, Springfield, Virginia 22151

MOTION SOFTWARE FOR A SYNERGISTIC SIX-DEGREE-OF-FREEDOM MOTION BASE

By Russell V. Parrish, James E. Dieudonne,
and Dennis J. Martin, Jr.*
Langley Research Center

SUMMARY

Computer software for the conversion of fixed-base simulations into moving-base simulations utilizing a synergistic six-degree-of-freedom motion simulator has been developed. This software includes an actuator extension transformation, inverse actuator extension transformation, a centroid transformation, and a washout circuit. Particular emphasis is placed upon the washout circuitry as adapted to fit the synergistic motion simulator. The description of the washout circuitry and illustration by means of a sample flight emphasize that translational cue representation may be of good fidelity, but care in the selection of parameters is very necessary, particularly in regard to anomalous rotational cues.

INTRODUCTION

The addition of the six-degree-of-freedom motion base to the simulation facilities of Langley Research Center is expected to enhance the quality of CTOL, STOL, and VTOL aircraft simulations. This particular base is synergistic in nature; the base does not have independent drive systems for each degree of freedom, but achieves motion in all degrees of freedom by a combination of actuator extensions. (See ref. 1.) The base will be integrated with normal fixed-base simulations into the real-time simulation facilities. (See ref. 2.) This paper will describe the general problem of converting existing fixed-base simulations into moving-base simulations and will place emphasis on the additional software required for the conversion to the particular base. The paper will introduce the necessary computer software including the actuator extension and inverse transformation described in reference 1, the centroid transformation, and the washout scheme, namely, the Langley adapted version of Schmidt and Conrad's coordinated washout circuitry (refs. 3 and 4).

Next, the motion limitations and restrictions of the Langley six-degree-of-freedom base will be presented, since these limitations are a major factor in the task suitability of

*Electronic Associates, Inc.

the particular base as well as in the selection of the parameters of the washout circuitry. The emphasis will be placed on the effects of the properties of the base on the software, including the selection of the neutral point and the prediction of the position constraints, dependent upon the current orientation (translational and rotational positions).

The remainder of the paper is devoted to the washout scheme, which, aside from the physical characteristics of the hardware, is the major factor affecting the quality of a motion simulation. Because of the complexity of Schmidt and Conrad's coordinated washout circuitry, a thorough explanation is necessary. The explanation proceeds from the general concept of the circuitry to the specific aspects of each component of the circuitry and concludes with a sample flight. The sample flight is included to depict the overall function of the circuitry and to illustrate the compromises necessary to keep the simulation within the base motion constraints while attempting to preserve the fidelity of the motion cues to the pilot.

SYMBOLS

Measurements and calculations were made in U.S. Customary Units. They are presented herein in the International System of Units (SI) with the equivalent values given parenthetically in the U.S. Customary Units.

A_1,A_2,A_3 acceleration lead parameters for translational channel lag compensation, sec^2

a_1,a_2,a_3 damping parameters for second-order translational washout filters, rad/sec

B_1,B_2,B_3 velocity lead parameters for translational channel lag compensation, sec

b_1,b_2,b_3 frequency parameters for second-order translational washout filters, rad/sec^2

C_1,C_2,C_3 translational acceleration braking parameters, per sec

$\vec{D}_i$ vector from moving coordinate system to upper attachment point of actuator i, m (ft)

$d_{i,j}$ jth element of vector $\vec{D}_i$

E_j,E_k intermediate terms in predicted limit calculation, m^2 (ft^2)

$\vec{F}_i$ vector from fixed floor coordinate system to lower point of attachment of actuator i

$f^*_{c,x}, f^*_{c,y}$ body-axis longitudinal and lateral accelerations at centroid location after low-pass filtering, m/sec^2 (ft/sec^2)

$f_{c,z}$ body-axis vertical acceleration (referenced about 1g) at centroid location after high-pass filtering, m/sec^2 (ft/sec^2)

$f_{i,x}, f_{i,y}, f_{i,z}$ inertial axis translational acceleration commands prior to translational washout, m/sec^2 (ft/sec^2)

$f^*_{i,x}, f^*_{i,y}$ inertial axis specific force error signals, m/sec^2 (ft/sec^2)

$f'_{i,x}, f'_{i,y}, f'_{i,z}$ components in inertial axis of filtered body-axis vertical acceleration at centroid location, m/sec^2 (ft/sec^2)

$f''_{i,z}$ artificial yaw error signal, m/sec^2 (ft/sec^2)

$f_{s,x}, f_{s,y}$ body-axis longitudinal and lateral accelerations at centroid location, m/sec^2 (ft/sec^2)

$f_{s,z}$ body-axis vertical acceleration (referenced about 1g) at centroid location, m/sec^2 (ft/sec^2)

f_x, f_y, f_z aircraft body axis translational accelerations, m/sec^2 (ft/sec^2)

$f_{x,c}, f_{y,c}, f_{z,c}$ body-axis translational accelerations at centroid location, m/sec^2 (ft/sec^2)

G_j, G_k intermediate terms in predicted limit calculation, m (ft)

g gravitational constant, m/sec^2 (ft/sec^2)

h integration step size in time, sec

i_o, j_o, k_o components of unit vectors defined in fixed-coordinate system

k_p, k_q, k_r scaling parameters for angular rates

$k_{p,T,1}, k_{q,T,1}, k_{r,1}$ parameters of signal-shaping network, per m (per ft)

$k_{p,T,2}, k_{q,T,2}, k_{r,2}$ parameters of signal-shaping network, sec

$k_{p,T,3}, k_{q,T,3}, k_{r,3}$ parameters of signal-shaping network, per sec

$k_{z,1}, k_{z,2}$ gain parameters of vertical channel high-pass filter

$k_{\theta,1}, k_{\theta,2}$ gain parameters of longitudinal channel low-pass filter

$k_{\phi,1}, k_{\phi,2}$ gain parameters of lateral channel low-pass filter

$k_{\psi,l}, k_{\theta,l}, k_{\phi,l}$ lead parameters for rotational channel lag compensation, sec

$\mathcal{L}(A,B)$ operator equal to $\begin{cases} \text{sgn } (A,B) & \text{when } |A| > B \\ A & \text{when } |A| \leq B \end{cases}$

$\vec{\ell}_i$ vector in fixed coordinate system from lower point of attachment to upper point of attachment of actuator i

ℓ_i magnitude of vector $\vec{\ell}_i$

p,q,r body-axis angular velocity commands, rad/sec

p',q',r' body-axis angular tilt velocity, rad/sec

p'',q'',r'' scaled body-axis aircraft angular velocities, rad/sec

p_a, q_a, r_a body-axis aircraft angular velocities, rad/sec

$\vec{R}$ vector from origin of fixed floor coordinate system to origin of moving coordinate system, m (ft)

R_x, R_y, R_z centroid location with respect to center of gravity, m (ft)

$\vec{r}_i$ vector of the fixed floor coordinate system to attachment point i in the moving coordinate system

s Laplace operator

T Euler angle transformation matrix for rotations about moving coordinate system

T_{ij} ith element in jth row of matrix T

t time, sec

V_ℓ velocity limit, m/sec (ft/sec)

x,y,z commanded inertial translational position of motion simulator, m (ft)

$\hat{x},\hat{y},\hat{z}$ commanded translational positions after compensation, m (ft)

$\ddot{x}_b,\ddot{y}_b,\ddot{z}_b$ intermediate inertial axis translational acceleration commands, m/sec^2 (ft/sec^2)

x_d,y_d,z_d inertial-axis translational position commands, m (ft)

x_{LF},y_{LF},z_{LF} scale factors on position limits

x_l,y_l,z_l inertial-axis position limits for translational channels, m (ft)

x_p,y_p,z_p coordinates of pilot's station with respect to center of gravity in body-axis system, m (ft)

$x_{p,c},y_{p,c},z_{p,c}$ coordinates of centroid location with respect to pilot's station in the body-axis system, m (ft)

z_{neut} actuator extension for selected neutral point, m (ft)

θ_j,ϕ_j values of trim tilt angles after j iterations, deg

θ_{j+1},ϕ_{j+1} values of trim tilt angles after j + 1 iterations, deg

$\xi_{z,1}$ damping parameter for vertical channel high-pass filter

ξ_θ,ξ_ϕ damping parameters of low-pass filters

τ parameter for trim option, m/sec (ft/sec)

ψ,θ,ϕ commanded inertial angular position of motion simulator, rad

$\hat{\psi},\hat{\theta},\hat{\phi}$ commanded angular positions after compensation, rad

$\dot{\psi}_T,\dot{\theta}_T,\dot{\phi}_T$ commanded inertial tilt rates, rad/sec

$\omega_{n,z,1}$ frequency parameter of vertical channel high-pass filter, rad/sec

$\omega_{n,\theta},\omega_{n,\phi}$ frequency parameters of low-pass filters, rad/sec

A dot over a variable indicates the time derivative of that variable. Superscript T denotes a transpose.

GENERAL PROBLEM

The conversion of a piloted aircraft simulation under fixed-base conditions to motion simulation requires the addition of several subroutines as depicted in figure 1. The first subroutine, the centroid transformation, converts translational accelerations (rotational rates need no transformation) occurring at the center of gravity of the simulated aircraft into translational accelerations which when applied at the centroid of the simulator, would produce the actual accelerations of the pilot's seat of the aircraft at the pilot's seat in the simulator. However, all motion simulators have limits on the amount of movement they allow in each degree of freedom. These limits, along with the number of degrees of freedom of allowable motion, vary with the design of motion simulators, but in all cases motion constraints exist. The design of a system or scheme which will transmit motion cues to a pilot while keeping the movement of the simulator within its constraints is the major task faced by the simulation analyst. After the cue has been transmitted, another function of this system, known as "washout," is to return the simulator to its neutral position without the pilot being aware of the movement. This tendency to keep the simulator near its neutral position maximizes the movement allowable for subsequent cues.

The output of the washout block shown in figure 1 is the position $(\hat{x},\hat{y},\hat{z})$ and angular orientation $\left(\hat{\psi},\hat{\theta},\hat{\phi}\right)$ of the centroid of the simulator. However, the design of the drive system of the Langley simulator requires a set of actuator extensions as inputs instead of $\hat{x}$, $\hat{y}$, $\hat{z}$, $\hat{\psi}$, $\hat{\theta}$, and $\hat{\phi}$. Therefore, the output of the washout scheme must be transformed into the proper format of actuator extensions before signals are sent to the simulator hardware.

The iterative scheme for calculating the inverse actuator transformation shown in the remaining starred block of figure 1 is used to monitor base position response. The addition of the centroid transformation, washout scheme, actuator extension transforma-

tion, and the inverse actuator transformation software to the standard fixed-base simulation should be sufficient in most cases for conversion from fixed to motion simulation.

SIX-DEGREE-OF-FREEDOM RESTRICTIONS

One basic problem in developing an adequate washout circuit for the subject six-degree-of-freedom motion base (see fig. 2) exists in handling motion constraints. The motion base is designed to give the pilot realistic motion in all six degrees of freedom but is subject to rigid performance limits. In each degree of freedom the motion base cannot exceed physical limits on position, velocity, and/or acceleration. These limits are given in table I from the manufacturer's specifications for a motion base "neutral point" of 0.61595 m (24.25 in.). The neutral point is the extension length of the six motion base actuators when the base is resting at its zero ($x = y = z = \psi = \theta = \phi = 0$) position. The position limits presented in table I are for motion in a single degree of freedom. However, because the actuators of the base may be extended only 1.524 m (60 in.), a displacement in one degree of freedom changes the maximum positions that may be obtained individually in each of the other five degrees of freedom. Table II shows how motion in one degree of freedom changes the maximum plus and minus positions that may be achieved individually in each of the other five degrees of freedom (based on empirical results). Because of the infinite number of possible combinations of displacements, a motion envelope for the subject base cannot be described. No position limit data are presented for cases beyond the interaction of two degrees of freedom.

The neutral point that is chosen can also affect the position limits. Each degree of freedom has a neutral point which will allow the maximum symmetric motion in that degree of freedom. These neutral points are given in table III.

A particular motion task may often require more motion in y and ϕ, or in z and θ, than in the other degrees of freedom. Such a task may require a neutral point which can provide for the maximum motion for the two degrees of freedom. In a straight-and-level flight the pilot feels a horizontal (x) force due to the pitch of the aircraft. For the transport used in the sample flight presented later, this force amounted to approximately 0.15g. A 8.5° tilt in pitch was necessary to achieve this sustained cue. Many motion tasks will need similar pitch angles. Table IV lists the preferred neutral points for heave motion with 6°, 8°, 10°, and 12° pitch angles.

As mentioned previously, the position limits of each degree of freedom change as the orientation of the base varies. Since the translational position limits play an important role in the operation of the washout, a method was developed, based on the inverse actuator transformation, to predict these limits based on the current orientation of the base. Essentially, the method predicts the limits of the translational channels through

conversion of the remaining travel of the currently longest and shortest actuators. (See appendix A.)

GENERAL CONCEPT OF THE WASHOUT CIRCUITRY

The function of the washout circuitry is to represent the translational accelerations and the rotational rates of the simulated aircraft. Motivation for the representation of rotational rates rather than rotation accelerations may be found in reference 3 (p. 6). Although a detailed explanation of the washout circuitry is presented in the next section, some discussion of the merits of coordination of translational and rotational motion is necessary. Sustained translational cues can only be represented on a motion simulator by tilting the pilot and utilizing the gravity vector to present the cue. However, the tilt angle must be obtained without pilot knowledge; that is, the rotation necessary to obtain the tilt angle should be made at a level below the pilot's sense threshold. Thus, the initial part of the cue, the onset, can only be represented by translational motion until the tilt angle is obtained. Thus, the coordination of translation and rotation is necessary.

In the case of a desired rotational cue, presentation of the onset cue by means of rotation alone results in a false translational cue because of temporary misalinement of the gravity vector. Thus, translational motion is required to offset the false cue induced by rotational motion. The concept of Schmidt and Conrad's coordinated washout is more easily illustrated with the block diagram presented in figure 3. As shown in the diagram, the translational forces at the center of gravity of the simulated aircraft are transformed to the centroid of the motion base, with regard to providing the desired motions at the pilot's station, prior to entrance of the washout circuitry. The motion of the base is then determined based on the desired motions of the centroid in the following manner:

The vertical acceleration $\ddot{z}_d$ is obtained, after preliminary filtering, by use of a second-order classical washout filter operating on the inertial vertical specific force.

The horizontal and lateral cues are obtained by separation of the low-frequency specific forces into steady-state and transient parts. The steady-state part of the cue is obtained by a tilt angle (θ representing sustained $\ddot{x}$, and ϕ representing sustained $\ddot{y}$) to aline the gravity vector. The transient part of the cue is obtained, through translational washout, in the form of second-order classical washout filters which are used to form the horizontal acceleration $\ddot{x}_d$ and the lateral acceleration $\ddot{y}_d$.

The application of braking accelerations, after the translational washout, is used to constrain further the translational motion in terms of acceleration, velocity, and position. The braking procedure is based on the position limits of the motion base which, in the case of the subject base, vary depending on the current orientation of the base and are provided by the predicted position limits.

No direct washout of the rotational degrees of freedom is provided. However, indirect washout is obtained through elimination of the false gravitational g cues that would be induced by a rotational movement. The onset and washout of the rotational movement is obtained with no false translational cues. As in the case of representation of a longitudinal or lateral cue by both tilt and translation, a rotational cue in ϕ or θ is represented by angular and translational motion. In this case, however, translational motion is used to eliminate the false g cue induced by the rotational movement. The translational movement makes no contribution to the rotational cue.

Indirect washout of the yaw angle ψ is accomplished by use of an artificial g cue in the manner of ϕ and θ degrees of freedom except that no translational movement is involved. After the desired position commands $\left(x_d,y_d,z_d,\psi,\theta,\phi\right)$ are obtained from the washout circuitry, compensation for base servo lag as determined from the response characteristics of the six-degree-of-freedom base (ref. 5) may be provided. The actuator extension transformation is then used to derive the proper actuator lengths that drive the motion base.

In summary, the concept of the coordinated washout circuitry is to represent longitudinal and lateral translational cues as completely as possible by utilizing both translational and rotational motions and to obtain rotational washout in a manner that preserves the fidelity of these translational cues.

MOTION SOFTWARE DESCRIPTION

In describing the motion software available for converting a fixed-base simulation to a moving-base simulation, major emphasis is placed on the centroid transformation and the washout circuitry rather than on the actuator extension transformation and the inverse actuator extension transformation. The emphasized parts of the software are illustrated in general form in figure 3 and in detailed form in figure 4. Frequent reference to figure 4 will be necessary inasmuch as the description of the software consists of a block-by-block discussion.

Centroid Transformation

The purpose of the centroid transformation is to provide the washout circuitry with the unconstrained motions of the base that would be necessary to produce all the cues to which a pilot would be subjected at the pilot's station. Thus, it is necessary to locate hypothetically the centroid of the motion base in the simulated aircraft with respect to the pilot's station, and then transform the motions, available at the center of gravity of the simulated aircraft, to this hypothetical location. The location with respect to the center of gravity is defined as

$$R_x = x_p + x_{p,c}$$

$$R_y = y_p + y_{p,c}$$

$$R_z = z_p + z_{p,c}$$

where x_p, y_p, and z_p locate the pilot's station with respect to the center of gravity and $x_{p,c}$, $y_{p,c}$, and $z_{p,c}$ locate the centroid with respect to the pilot's station. Once the centroid location is determined, the translational forces are transformed to the centroid by

$$f_{x,c} = f_x - \left(q_a^2 + r_a^2\right)R_x + \left(q_a p_a - \dot{r}_a\right)R_y + \left(r_a p_a + \dot{q}_a\right)R_z$$

$$f_{y,c} = f_y + \left(p_a q_a + \dot{r}_a\right)R_x - \left(p_a^2 + r_a^2\right)R_y + \left(r_a q_a - \dot{p}_a\right)R_z$$

$$f_{z,c} = f_z + \left(p_a r_a - \dot{q}_a\right)R_x + \left(q_a r_a + \dot{p}_a\right)R_y - \left(p_a^2 + q_a^2\right)R_z$$

No transformation of the angular rates is necessary.

Washout Circuitry

After transforming the desired motions to the base centroid, it is necessary to constrain these motions to be within the physical capabilities of the motion base and still maintain the fidelity of the motion cues provided to the pilot. This is the purpose of the washout circuitry, which will now be described block by block in accordance with figure 4. The detailed equations are presented in appendix B.

The normal acceleration in the body-axis system is first divided into two parts; the normal-force variations from 1g, $f_{s,z}$, and a constant 1g normal force. High-pass filtering of $f_{s,z}$ then removes the low-frequency components likely to exceed the motion base position limits. No tilt angle is available to represent this part of the normal-force variation, and thus it cannot be reproduced. The high-pass filter used for this purpose is the second-order classical filter

$$f_{c,z} = \frac{1}{k_{z,2}}\left(k_{z,1}f_{s,z} - 2\xi_{z,1}\omega_{n,z,1}\int f_{c,z}\,dt - \omega_{n,z,1}^2\iint f_{c,z}\,dt\,dt\right)$$

After filtering the normal-force variations from 1g, the resulting signal $f_{c,z}$ is transformed to inertial coordinates before further operation.

The longitudinal and lateral forces, in the body-axis system, are filtered to remove the higher frequency components from which undesirable angular rate responses result. This procedure is not necessary for the normal force since it is not coordinated with a tilt angle. The low-pass filters used for this purpose are the second-order classical filters

$$\ddot{f}^*_{c,x} = k_{\theta,1}\omega^2_{n,\theta}f_{s,x} - 2\xi_\theta\omega_{n,\theta}\dot{f}^*_{c,x} - \omega^2_{n,\theta}f^*_{c,x}$$

$$\ddot{f}^*_{c,y} = k_{\phi,1}\omega^2_{n,\phi}f_{s,y} - 2\xi_\phi\omega_{n,\phi}\dot{f}^*_{c,x} - \omega^2_{n,\phi}f^*_{c,y}$$

The resulting signals, $f^*_{c,x}$ and $f^*_{c,y}$, along with the constant 1g normal force, are then transformed to inertial coordinates to form the specific force error signals. These error signals are used to coordinate the tilt angles (representing sustained forces) and the translational movement (representing transient forces).

The translational part of the longitudinal and lateral specific forces are obtained prior to translational washout by the summing of the specific force error signals with the normal-force components in the inertial system. This summation results in the totally transformed longitudinal and lateral specific forces, $f_{i,x}$ and $f_{i,y}$, respectively, in the inertial-axis system. It should be noted that the body-axis system contributions of $f^*_{c,x}$ and $f^*_{c,y}$ to the inertial-axis system $f_{i,z}$ have been neglected because of the low-frequency content of these contributions. Also, these contributions are small as long as θ and ϕ are small.

The tilt angle part of the longitudinal and lateral specific forces are also obtained, along with the inertial washout of the rotational channels, through the use of the specific force error signals. The error signals are used to feed back base attitude information to the signal shaping network. This network is multipurpose in that it is used: (1) to produce the angular rates necessary to achieve the tilt angles; (2) to constrain the position drives x and y by apportioning the sustained and transient forces between rotational and translational degrees of freedom; (3) to eliminate the false specific force cues induced by rotational movement with the translation commanded by $f^*_{i,x}$ and $f^*_{i,y}$; and (4) to provide the washout of the rotational channels by use of the feedback error signals $f^*_{i,x}$ and $f^*_{i,y}$ generated by the false specific force cues induced by rotation. Naturally, compromises are necessary in the selection of the parameters of this network in order to serve all of these purposes. Parameters selected to constrain the x and y position drives usually will produce large angular rates for tilts; thus, large anomalous rotational cues

are induced and may provide insufficient washout properties for rotational channels. Conversely, parameters selected and based on rotational properties usually will not constrain the x and y position drives sufficiently.

The resulting signals formed by the signal shaping network, $\dot{\phi}_T$, $\dot{\theta}_T$, and $\dot{\psi}_T$, must be transformed from the inertial system to the body-axis system, and then summed with the scaled angular rates of the aircraft. The resultant angular rates are then transformed back to the inertial-axis system to provide the angular drive commands.

An artificial signal, $f''_{i,z} = -g\psi$, is used to provide the washout of the yaw channel. In this case, the parameters of the signal shaping network can be chosen wholly on the basis of the yaw channel washout, inasmuch as no coordination with translational channels is necessary.

A trim option is available to insure that any initial sustained specific forces in x and y can be obtained with tilts prior to the initiation of a simulated flight. The option requires the following initial conditions on the x and y low-pass filters:

$$f^*_{c,x}(0) = \frac{k_{\theta,1} f_{s,x}(0)}{\omega^2_{n,\theta}}$$

$$f^*_{c,y}(0) = \frac{k_{\phi,1} f_{s,y}(0)}{\omega^2_{n,\phi}}$$

These initial conditions provide specific force error signals that are used to iterate to the trim tilt angles in the hold mode of the real-time system, by utilizing the following iterative equations:

$$\theta_{j+1} = \theta_j + f^*_{i,x} \frac{h}{\tau}$$

$$\phi_{j+1} = \phi_j + f^*_{i,y} \frac{h}{\tau}$$

Translational washout of the inertial x, y, and z degrees of freedom is carried out on the previously generated signals $f_{i,x}$, $f_{i,y}$, and $f_{i,z}$, respectively. Schmidt and Conrad included this inertial washout because the body-axis washout of the inertial channel (the z high-pass filter) does not guarantee a bounding of the inertial position command. Also, the signal shaping network, although used to constrain the longitudinal and

lateral degrees of freedom, is not sufficient for washout of the inertial x and y channels. The translational washout is achieved by use of second-order classical washout filters of the form

$$\ddot{x}_d = f_{i,x} - a_1\dot{x}_d - b_1 x_d$$

$$\ddot{y}_d = f_{i,y} - a_2\dot{y}_d - b_2 y_d$$

$$\ddot{z}_d = f_{i,z} - a_3\dot{z}_d - b_3 z_d$$

As pointed out previously, a braking acceleration procedure is included to augment the washout of the translational degrees of freedom. The procedure consists of limiting acceleration commands above the capabilities of the base to the acceleration limits, and also of maintaining the position limits by means of a position-velocity boundary. The position-velocity boundary based on the acceleration limit, the position limit, and the current position of the base is determined. The braking procedure will be illustrated for the positive case of the horizontal degree of freedom. The positive velocity limit at the boundary is defined as

$$\dot{x}_l = \sqrt{2\ddot{x}_l\left(x_l - x_d\right)}$$

The value of the computed velocity limit is then forced within the base specification velocity limit of 0.61 m/sec (2 ft/sec). Once the velocity limit is determined, braking is achieved whenever either the position limit or the computed velocity limit is exceeded with the drive commands by recomputing the acceleration command signal as

$$\ddot{x}_b = \ddot{x}_d - C_1\left(\dot{x}_d - \dot{x}_l\right)$$

Thus, when the velocity limit is exceeded by the commanded velocity, braking occurs to reduce the velocity to the velocity limit.

When the base is at the position limit,

$$x_l = x_d$$

$$\dot{x}_l = 0$$

the acceleration command signal is recomputed to be

$$\ddot{x}_b = \ddot{x}_d - C_1\dot{x}_d$$

and braking occurs to null both the acceleration and the velocity.

Since the subject base has variable position limits, some provision must be made to supply the current translational position limits, determined by the base orientation, to the braking acceleration procedure. Because of the highly nonlinear nature of the equations governing the current position limits, only predictions of the position limits are supplied by the motion software. These predictions are determined from the longest and shortest actuator extensions present at the time of the prediction. (See appendix A.) These predictions are considered to be sufficient for the purpose, and have worked well in test cases.

With the completion of the braking procedure, the constrained translational cues are available to drive the motion base, along with the rotational cues provided by the coupling of the lateral and longitudinal motions with the scaled angular rates. Provision has been made for the addition of lead to all the drive channels in the software in order to compensate for the servo lag of the six-degree-of-freedom base (ref. 5).

The motion software package is then complete except for some means of monitoring how well the washout is doing. The following equations are available to transform the inertial translational cues, along with gravity cues, back into the body axis for comparison with $f_{x,c}$, $f_{y,c}$, and $f_{z,c}$:

$$\hat{\ddot{x}} = \ddot{x}_d(\cos\theta\cos\psi) + \ddot{y}_d(\cos\theta\sin\psi) - \left(\ddot{z}_d - g\right)(\sin\theta)$$

$$\hat{\ddot{y}} = \ddot{x}_d(\sin\phi\sin\theta\cos\psi - \sin\psi\cos\phi) + \ddot{y}_d(\sin\phi\sin\theta\sin\psi + \cos\phi\cos\psi) + \left(\ddot{z}_d - g\right)(\sin\phi\cos\theta)$$

$$\hat{\ddot{z}} = \ddot{x}_d(\cos\phi\sin\theta\cos\psi + \sin\phi\sin\psi) + \ddot{y}_d(\cos\phi\sin\theta\sin\psi - \sin\phi\cos\psi) + \left(\ddot{z}_d - g\right)(\cos\phi\cos\theta)$$

No transformation is necessary for the rotational channels since p, q, and r are readily available.

SAMPLE FLIGHT

In order to demonstrate the use of the motion software on the Langley six-degree-of-freedom motion base, a representative flight was made with a fixed-base simulation of a DC-8/707 class transport. The flight consisted of an elevator doublet input followed by an aileron doublet input and concluded with a rudder doublet input. The resulting motions of the center of gravity were placed on tape and later used to drive the motion software and the six-degree-of-freedom motion base. It must be emphasized that the parameters used in the software (table V) are by no means values that are recommended for motion simulation, but merely values that constrain the motions to remain within the position limits of the base.

The taped variables were fed through the centroid transformation, the washout, and the actuator extension transformation into the six-degree-of-freedom base. The actuator extensions of the base were then fed into the inverse transformation to monitor the base response. Figure 5 shows a comparison of $f_{x,c}$, $f_{y,c}$, and $f_{z,c}$ and p_a, q_a, and r_a of the airplane at the hypothetical centroid location with the commanded motion cues. The density of the time-history comparison is $2\frac{2}{7}$ points per second for the flight data and 16 points per second for the washout commands. A discussion of each of the six channels follows:

Because the aircraft configuration used in the sample flight trims in a nose-up attitude of about 8.5° for straight and level flight at the selected airspeed, the horizontal force has a sustained value of about 0.15g. This part of the cue is obtained by a pitch tilt. The higher frequency variation about this value is obtained by horizontal translations. As may be seen, good fidelity of the horizontal force cue is obtained.

Although fair fidelity of the pitch rate cue is obtained, an anomalous rotational cue used to control the tilt portion of the horizontal force is present at $t \approx 35$ sec.

Because of the limited amount of travel available in heave when a pitch angle is present, good fidelity of the vertical force channel is not achieved. The time-history comparison of this channel illustrates problems common to classical filters, namely, phase shift and the magnitude of the washout. In the case of this channel, often the washout is larger than the onset cue.

The fact that rotational fidelity may be sacrificed to improve translational cues is dramatically illustrated by this comparison of roll rate. Most of the roll rate has been devoted to controlling the g side force rather than the roll rate of the airplane.

Good fidelity of the lateral force cue is obtained by use of the roll tilt angle and lateral translation.

A fair representation of the yaw rate is achieved since the yaw angle can make no contribution to a translational cue.

Figure 6 shows a comparison of the six commanded positions of the base with the actual base response obtained. It should be noted that an additional lag of 1/32 second has been introduced into the comparison because of a sampling delay necessary to supply the inverse actuator extension transformation with the actual extensions of the base actuators.

A discussion of each channel is probably not necessary. However, it is interesting to note that the return of the translational channels to the neutral point is very slow; thus, the available travel for subsequent cues is restricted. Also, the sustained pitch angle of 8.5^{o} is evident throughout the run, and, at $t \approx 26$ sec, an acceleration limit of the hardware's pitch channel has apparently been exceeded.

CONCLUDING REMARKS

The addition of the computer software described in this report to existing and future fixed-base simulations should minimize the efforts in the conversion to moving-base simulations. The general problem of conversion has been discussed as well as the limitations and restrictions of the existing hardware as these restrictions apply to the problem. The description and illustration by means of a sample flight of the washout circuitry emphasize that translational cue representation may be of good fidelity, although care in the selection of parameters is very necessary, particularly in regard to anomalous rotational cues.

Langley Research Center,
National Aeronautics and Space Administration,
Hampton, Va., September 4, 1973.

APPENDIX A

METHOD FOR PREDICTING POSITION LIMITS

Reference 1 gives the equation of each actuator $\left(\vec{\ell}_i\right)$ as a function of the base dimensions and the current base position as

$$\vec{\ell}_i = [T]\vec{D}_i + \vec{R} - \vec{F}_i \tag{A1}$$

where $[T]$ is the Euler angle transformation matrix for rotations about the moving coordinate system

$$[T] = \begin{bmatrix} \cos\psi\cos\theta & \cos\psi\sin\theta\sin\phi - \sin\psi\cos\phi & \cos\psi\sin\theta\cos\phi + \sin\psi\sin\phi \\ \sin\psi\cos\theta & \sin\psi\sin\theta\sin\phi + \cos\psi\cos\phi & \sin\psi\sin\theta\cos\phi - \cos\psi\sin\phi \\ -\sin\theta & \cos\theta\sin\phi & \cos\theta\cos\phi \end{bmatrix} \tag{A2}$$

$\vec{D}_i$ is the vector from the moving coordinate system to the upper attachment point of actuator i, $\vec{F}_i$ is the vector from the fixed floor coordinate system to the lower point of attachment of actuator i, and $\vec{R}$ is the vector from the fixed floor coordinate system to the origin of the moving coordinate system. (See fig. 7.)

Multiplying $\vec{\ell}_i$ by its transpose $\vec{\ell}_i^T$ generates an equation in terms of the scalar actuator length ℓ_i

$$\vec{\ell}_i^T\vec{\ell}_i = \left\{[T]\vec{D}_i + \vec{R} - \vec{F}_i\right\}^T\left\{[T]\vec{D}_i + \vec{R} - \vec{F}_i\right\} \tag{A3}$$

Equation (A3) may be expanded and simplified as

$$\left|\vec{\ell}_i\right|^2 = \vec{\ell}_i^T\vec{\ell}_i = \vec{D}_i^T[T]^T[T]\vec{D}_i + \vec{D}_i^T[T]^T\vec{R} - \vec{D}_i^T[T]^T\vec{F}_i + \vec{R}^T[T]\vec{D}_i + \vec{R}^T\vec{R} - \vec{R}^T\vec{F}_i - \vec{F}_i^T[T]\vec{D}_i - \vec{F}_i^T\vec{R} + \vec{F}_i^T\vec{F}_i \tag{A4}$$

$$\left|\vec{\ell}_i\right|^2 = D_i^2 + \vec{D}_i^T[T]^T\vec{R} - \vec{D}_i^T[T]^T\vec{F}_i + \vec{R}^T[T]\vec{D}_i + R^2 - \vec{R}^T\vec{F}_i - \vec{F}_i^T[T]\vec{D}_i - \vec{F}_i^T\vec{R} + F_i^2 \tag{A5}$$

$$\left|\vec{\ell}_i\right|^2 = d_{1,i}^2 + d_{2,i}^2 + d_{3,i}^2 + \begin{bmatrix} d_{1,i} & d_{2,i} & d_{3,i} \end{bmatrix} \begin{bmatrix} T_{11} & T_{21} & T_{31} \\ T_{12} & T_{22} & T_{32} \\ T_{13} & T_{23} & T_{33} \end{bmatrix} \begin{bmatrix} x \\ y \\ z \end{bmatrix} - \begin{bmatrix} d_{1,i} & d_{2,i} & d_{3,i} \end{bmatrix} \begin{bmatrix} T_{11} & T_{21} & T_{31} \\ T_{12} & T_{22} & T_{32} \\ T_{13} & T_{23} & T_{33} \end{bmatrix} \begin{bmatrix} f_{1,i} \\ f_{2,i} \\ f_{3,i} \end{bmatrix}$$

$$+ \begin{bmatrix} x & y & z \end{bmatrix} \begin{bmatrix} T_{11} & T_{12} & T_{13} \\ T_{21} & T_{22} & T_{23} \\ T_{31} & T_{32} & T_{33} \end{bmatrix} \begin{bmatrix} d_{1,i} \\ d_{2,i} \\ d_{3,i} \end{bmatrix} + x^2 + y^2 + z^2 - \begin{bmatrix} x & y & z \end{bmatrix} \begin{bmatrix} f_{1,i} \\ f_{2,i} \\ f_{3,i} \end{bmatrix} - \begin{bmatrix} f_{1,i} & f_{2,i} & f_{3,i} \end{bmatrix} \begin{bmatrix} T_{11} & T_{12} & T_{13} \\ T_{21} & T_{22} & T_{23} \\ T_{31} & T_{32} & T_{33} \end{bmatrix} \begin{bmatrix} d_{1,i} \\ d_{2,i} \\ d_{3,i} \end{bmatrix}$$

$$- \begin{bmatrix} f_{1,i} & f_{2,i} & f_{3,i} \end{bmatrix} \begin{bmatrix} x \\ y \\ z \end{bmatrix} + f_{1,i}^2 + f_{2,i}^2 + f_{3,i}^2 \qquad \text{(A6)}$$

To give a scalar equation for ℓ_i^2 in terms of current base position coordinates (x,y,z,ψ,θ,ϕ) and base dimension coordinates $\left(d_{i,j},f_{i,j}\right)$. Equation (A6) can be expanded and reordered to yield

$$\left|\vec{\ell}_i\right|^2 = x^2 + 2x\left\{d_{1,i}T_{11} + d_{2,i}T_{21} + d_{3,i}T_{31} - f_{1,i}\right\} + y^2 + 2y\left\{d_{1,i}T_{12} + d_{2,i}T_{22} + d_{3,i}T_{32} - f_{2,i}\right\} + z^2 + 2z\left\{d_{1,i}T_{13} + d_{2,i}T_{23} + d_{3,i}T_{33} - f_{3,i}\right\} + d_{1,i}^2 + d_{2,i}^2 + d_{3,i}^2 + f_{1,i}^2 + f_{2,i}^2 + f_{3,i}^2 - 2f_{1,i}\left\{d_{1,i}T_{11} + d_{2,i}T_{21} + d_{3,i}T_{31}\right\} - 2f_{2,i}\left\{d_{1,i}T_{12} + d_{2,i}T_{22} + d_{3,i}T_{32}\right\} - 2f_{3,i}\left\{d_{1,i}T_{13} + d_{2,i}T_{23} + d_{3,i}T_{33}\right\} \qquad \text{(A7)}$$

There are rigid upper and lower limits on the available motion in x, y, and z due to the physical dimensions of the motion base. Each of the six actuators may extend to a length of 4.1402 m (13.5833 ft) and retract to a length of 2.6162 m (8.5833 ft). The amount of available motion in one degree of freedom at any point in time is a function of the values of the other five degrees of freedom at that time. A motion excursion limit is reached when the commanded position (x,y,z,ψ,θ,ϕ) produces an actuator length $\left|\vec{\ell}_i\right|(x,y,z,\psi,\theta,\phi)$ (eq. (A7)) which exceeds the rigid actuator length constraints $\left(2.6162 \text{ m} \leqq \left|\vec{\ell}_i\right| \leqq 4.1402 \text{ m}\right)$. A prediction of the motion limits for x, y, and z may be obtained using equation (A7) for the longest and shortest actuator at that time.

For example, to determine the predicted limit for x, j is chosen such that $\left|\vec{\ell}_j\right| \geqq \left|\vec{\ell}_i\right|$ (where i = 1,6). Fixing the other five degrees of freedom (y,z,ψ,θ,ϕ) to their values at that time, equation (A7) can be rewritten as

$$x^2 + 2G_j x + E_j = \left|\vec{\ell}_j\right|^2 \tag{A8}$$

where

$$G_j = G_j(\psi,\theta,\phi) \tag{A9}$$

$$E_j = E_j(y,z,\psi,\theta,\phi) \tag{A10}$$

Equation (A8) is a simple quadratic in x. Setting $\left|\vec{\ell}_j\right|$ to its maximum length (4.1402 m (13.5833 ft)), equation (A8) may be solved to yield the value for x when the longest actuator has reached full extension. Equation (A8) has one positive root and one negative root. (Because of the motion limitations of the base, the y, z, ψ, θ, and ϕ configuration for which eq. (A8) has two positive roots or two negative roots cannot be achieved.) If the x velocity is positive, x is increasing in value toward the positive x position which causes the longest actuator to be fully extended. In this case the positive root is chosen. Similarly, if the x velocity is negative, the negative root is chosen.

Next, k is chosen so that $\left|\vec{\ell}_k\right| < \left|\vec{\ell}_i\right|$ (where $i = 1,6$). Equation (A8) is again used, this time for the shortest actuator ℓ_k,

$$x^2 + 2G_k x + E_k = \left|\vec{\ell}_k\right|^2 \tag{A11}$$

By setting ℓ_k to its shortest possible extension (2.6162 m (8.5833 ft)) equation (A11) may be solved for x. Again, the solution is chosen that has the same sign as the x velocity.

Thus two predicted values for the maximum available excursion in x may exist, one based upon the x value when the longest actuator reaches maximum extension, and one based upon the x value when the shortest actuator reaches minimum extension. These two values are compared with a standard x limit value and the smallest (in absolute value) of the three is chosen for the x limit.

In some y, z, ψ, θ, and ϕ configurations, a real x value may not exist which drives the longest actuator to full extension or drives the shortest actuator to minimum extension. In such a case the imaginary solutions obtained are not considered.

The same method is used to predict the limits for y and z.

APPENDIX B

DETAILED EQUATIONS FOR THE WASHOUT CIRCUIT

The following is a block-by-block list of equations corresponding to figure 4:

Centroid transformation:

$$R_x = x_p + x_{p,c}$$

$$R_y = y_p + y_{p,c}$$

$$R_z = z_p + z_{p,c}$$

$$f_{s,x} = f_x - \left(q_a^2 + r_a^2\right)R_x + \left(q_a p_a - \dot{r}_a\right)R_y + \left(r_a p_a + \dot{q}_a\right)R_z$$

$$f_{s,y} = f_y + \left(p_a q_a + \dot{r}_a\right)R_x - \left(p_a^2 + r_a^2\right)R_y + \left(r_a q_a - \dot{p}_a\right)R_z$$

$$f_{z,c} = f_z + \left(p_a q_a - \dot{q}_a\right)R_x + \left(q_a r_a + \dot{p}_a\right)R_y - \left(p_a^2 + q_a^2\right)R_z$$

Variation about 1g:

$$f_{s,x} = f_{x,c} + g$$

High-pass filter:

$$f_{c,z} = \frac{k_{z,1} f_{s,z} - 2\xi_{z,1}\omega_{n,z,1}\int f_{c,z}\,dt - \omega_{n,z,1}^2 \iint f_{c,z}\,dt\,dt}{k_{z,2}}$$

Low-pass filter:

$$\ddot{f}^*_{c,x} = k_{\theta,1}\omega_{n,\theta}^2 f_{s,x} - 2\xi_\theta \omega_{n,\theta}\dot{f}^*_{c,x} - \omega_{n,\theta}^2 f^*_{c,x}$$

$$\ddot{f}^*_{c,y} = k_{\phi,1}\omega_{n,\phi}^2 f_{s,y} - 2\xi_\phi \omega_{n,\phi}\dot{f}^*_{c,x} - \omega_{n,\phi}^2 f^*_{c,y}$$

Body to inertial transformation, high-frequency components:

$$f'_{i,x} = f_{c,z}(\cos\phi \sin\theta \cos\psi + \sin\phi \sin\psi)$$

$$f'_{i,y} = f_{c,z}(\cos\phi \sin\theta \sin\psi - \sin\phi \cos\psi)$$

$$f'_{i,z} = f_{c,z}(\cos\phi \cos\theta)$$

Body to inertial transformation, low-frequency components:

$$f^*_{i,x} = f^*_{c,x}(\cos\theta \cos\psi) + f^*_{c,y}(\sin\phi \sin\theta \cos\psi - \cos\phi \sin\psi) - g(\cos\phi \sin\theta \cos\psi + \sin\phi \sin\psi)$$

$$f^*_{i,y} = f^*_{c,x}(\cos\theta \sin\psi) + f^*_{c,y}(\sin\phi \sin\theta \sin\psi + \cos\phi \cos\psi) - g(\cos\phi \sin\theta \sin\psi - \sin\phi \cos\psi)$$

Sum of low- and high-frequency components:

$$f_{i,x} = f'_{i,x} + f^*_{i,x}$$

$$f_{i,y} = f'_{i,y} + f^*_{i,y}$$

$$f_{i,z} = f'_{i,z}$$

Signal-shaping network:

$$\dot{\theta}_T = k_{q,T,1}k_{q,T,2}\dot{f}^*_{i,x} + k_{q,T,1}\int f^*_{i,x}\,dt + k_{q,T,1}k_{q,T,3}\iint f^*_{i,x}\,dt\,dt$$

$$\dot{\phi}_T = -k_{p,T,1}k_{p,T,2}\dot{f}^*_{i,y} - k_{p,T,1}\int f^*_{i,y}\,dt - k_{p,T,1}k_{p,T,3}\iint f^*_{i,y}\,dt\,dt$$

$$\dot{\psi}_T = k_{r,1}k_{r,2}\dot{f}''_{i,z} + k_{r,1}\int f''_{i,z}\,dt + k_{r,1}k_{r,3}\iint f''_{i,z}\,dt\,dt$$

Inertial to body transformation:

$$p' = \dot{\phi}_T(\cos\theta\cos\psi) + \dot{\theta}_T(\cos\theta\sin\psi) - \dot{\psi}_T(\sin\theta)$$

$$q' = \dot{\phi}_T(\sin\phi\sin\theta\cos\psi - \cos\phi\sin\psi) + \dot{\theta}_T(\sin\phi\sin\theta\sin\psi + \cos\phi\cos\psi) + \dot{\psi}_T(\sin\phi\cos\theta)$$

$$r' = \dot{\phi}_T(\cos\phi\sin\theta\cos\psi + \sin\phi\sin\psi) + \dot{\theta}_T(\cos\phi\sin\theta\sin\psi - \sin\phi\cos\psi) + \dot{\psi}_T(\cos\phi\cos\theta)$$

Scale airplane angular rates:

$$p'' = k_p p_a$$

$$q'' = k_q q_a$$

$$r'' = k_r r_a$$

Sum of airplane and tilt rates:

$$p = p'' + p'$$

$$q = q'' + q'$$

$$r = r'' + r'$$

Transformation to Euler rates:

$$\dot{\phi} = p + q\sin\phi\tan\theta + r\cos\phi\tan\theta$$

$$\dot{\theta} = q\cos\phi - r\sin\phi$$

$$\dot{\psi} = (q\sin\phi + r\cos\phi)\sec\theta$$

Angular lead compensation:

$$\hat{\psi} = \psi + k_{\psi,l}\dot{\psi}$$

$$\hat{\theta} = \theta + k_{\theta,l}\dot{\theta}$$

$$\hat{\phi} = \phi + k_{\phi,l}\dot{\phi}$$

Translational lead compensation:

$$\hat{x} = x_d + A_1\ddot{x}_d + B_1\dot{x}_d$$

$$\hat{y} = y_d + A_2\ddot{y}_d + B_2\dot{y}_d$$

$$\hat{z} = z_d + A_3\ddot{z}_d + B_3\dot{z}_d$$

Translational washout:

$$\ddot{x}_d = f_{i,x} - a_1\dot{x}_d - b_1x_d$$

$$\ddot{y}_d = f_{i,y} - a_2\dot{y}_d - b_2y_d$$

$$\ddot{z}_d = f_{i,z} - a_3\dot{z}_d - b_3z_d$$

Limit prediction based on current position:

See appendix A for equations and derivation.

REFERENCES

1. Dieudonne, James E.; Parrish, Russell V.; and Bardusch, Richard E.: An Actuator Extension Transformation for a Motion Simulator and an Inverse Transformation Applying Newton-Raphson's Method. NASA TN D-7067, 1972.

2. Grove, Randall D.; and Mayhew, Stanley C.: A Real-Time Digital Program for Estimating Aircraft Stability and Control Parameters From Flight Test Data by Using the Maximum Likelihood Method. NASA TM X-2788, 1973.

3. Schmidt, Stanley F.; and Conrad, Bjorn: Motion Drive Signals for Piloted Flight Simulators. NASA CR-1601, 1970.

4. Schmidt, Stanley F.; and Conrad, Bjorn: A Study of Techniques for Calculating Motion Drive Signals for Flight Simulators. Rep. No. 71-28, Analytical Mechanics Associates, Inc., July 1971. (Available as NASA CR-114345.)

5. Parrish, Russell V.; Dieudonne, James E.; Martin, Dennis J., Jr.; and Copeland, James L.: Compensation Based on Linearized Analysis for a Six-Degree-of-Freedom Motion Simulator. NASA TN D-7349, 1973.

TABLE I.- PERFORMANCE LIMITS

Degree of freedom	Performance limits		
	Position	Velocity	Acceleration
Horizontal x	Forward 1.245 m Aft 1.219 m	±0.610 m/sec	±0.6g
Lateral y	Left 1.219 m Right 1.219 m	±0.610 m/sec	±0.6g
Vertical z	Up 0.991 m Down .762 m	±0.610 m/sec	±0.6g
Yaw ψ	±32°	±15°/sec	±50°/sec^2
Pitch θ	+30° -20°	±15°/sec	±50°/sec^2
Roll ϕ	±22°	±15°/sec	±50°/sec^2

TABLE II.- POSITION LIMITS OF THE OTHER FIVE DEGREES OF FREEDOM FOR A STATIC POSITION OF THE SIXTH DEGREE OF FREEDOM

(a) The horizontal degree of freedom x

x static position, m	Position limits				
	y, m	z, m	ψ, deg	θ, deg	ϕ, deg
1.016	0.7813	0.1351	10.96	7.65	4.18
	-.7813	-.5220	-10.96	-23.52	-4.18
0.762	1.0196	0.2504	17.40	13.78	7.81
	-1.0196	-.7018	-17.40	-31.29	-7.81
0.508	1.1676	0.4018	24.06	21.20	12.73
	-1.1676	-.8534	-24.06	-27.55	-12.73
0.254	1.2484	0.5977	30.94	29.73	19.54
	-1.2484	-.9804	-30.94	-24.56	-19.54
0.0	1.3071	0.8537	38.15	32.19	24.03
	-1.3071	-1.0848	-38.15	-22.39	-24.03
-0.254	1.3449	0.6792	31.39	32.54	19.61
	-1.3449	-.9362	-31.39	-21.09	-19.61
-0.508	1.2865	0.5519	23.38	32.32	16.24
	-1.2865	-.7610	-23.38	-20.72	-16.24
-0.762	1.2502	0.4630	15.53	26.46	13.81
	-1.2502	-.5552	-15.53	-21.44	-13.81
-1.016	0.9411	0.4082	7.90	22.13	9.51
	-.9411	-.3124	-7.90	-23.56	-9.51

TABLE II.- POSITION LIMITS OF THE OTHER FIVE DEGREES OF FREEDOM FOR A STATIC POSITION OF THE SIXTH DEGREE OF FREEDOM – Continued

(b) The lateral degree of freedom y

y static position, m	Position limits				
	x, m	z, m	ψ, deg	θ, deg	ϕ, deg
1.016	0.7663 -.9241	0.1562 -.3302	7.96 -14.21	9.15 -4.20	23.45 -10.88
0.762	1.0345 -1.0919	0.2670 -.5674	15.16 -21.34	16.01 -7.15	25.64 -12.89
0.508	1.2504 -1.1791	0.4138 -.7686	22.73 -28.03	22.07 -11.00	25.50 -15.77
0.254	1.3515 -1.2438	0.6043 -.9398	30.79 -33.44	27.44 -15.95	26.77 -19.49
0.0	1.4935 -1.2873	0.8537 -1.0848	38.15 -38.15	32.19 -22.39	24.03 -24.03
-0.254	1.3515 -1.2438	0.6043 -.9398	33.44 -30.79	27.44 -15.95	19.49 -26.77
-0.508	1.2504 -1.1791	0.4138 -.7686	28.03 -22.73	22.07 -11.00	15.77 -25.50
-0.762	1.0345 -1.0919	0.2670 -.5674	21.34 -15.16	16.01 -7.15	12.89 -25.64
-1.016	0.7663 -.9241	0.1562 -.3302	14.21 -7.96	9.15 -4.20	10.88 -23.45

TABLE II.- POSITION LIMITS OF THE OTHER FIVE DEGREES OF FREEDOM FOR A STATIC POSITION OF THE SIXTH DEGREE OF FREEDOM – Continued

(c) The vertical degree of freedom z

z static position, m	Position limits				
	x, m	y, m	ψ, deg	θ, deg	ϕ, deg
0.762	0.0828 -.1237	0.0851 -.0851	2.27 -2.27	4.85 -2.47	2.83 -2.83
0.508	0.3622 -.6213	0.3741 -.3741	9.77 -9.77	17.73 -9.16	10.31 -10.31
0.254	0.7551 -1.4224	0.7882 -.7882	19.99 -19.99	28.40 -15.74	17.28 -17.28
0.0	1.4935 -1.2873	1.3071 -1.3071	38.15 -38.15	32.19 -22.39	24.03 -24.03
-0.254	1.3277 -1.0711	1.0889 -1.0889	32.06 -32.06	23.94 -29.29	25.54 -25.54
-0.508	1.0338 -.8148	0.8298 -.8298	23.81 -23.81	16.23 -27.95	17.64 -17.64
-0.762	0.6668 -.5067	0.5169 -.5169	14.43 -14.43	8.91 -15.87	9.86 -9.86
-1.016	0.1730 -.1229	0.1260 -.1260	3.41 -3.41	1.88 -3.49	2.11 -2.11

TABLE II.- POSITION LIMITS OF THE OTHER FIVE DEGREES OF FREEDOM FOR A STATIC POSITION OF THE SIXTH DEGREE OF FREEDOM – Continued

(d) The yaw degree of freedom ψ

ψ static position, deg	Position limits				
	x, m	y, m	z, m	θ, deg	ϕ, deg
30	0.2880 -.2977	0.2781 -.4290	0.0859 -.3203	4.45 -2.34	2.74 -2.65
20	0.6619 -.6167	0.5979 -.8108	0.2537 -.6154	13.92 -6.90	7.99 -7.97
10	1.0551 -.9456	0.9428 -1.1610	0.5014 -.8694	25.77 -13.53	15.22 -16.28
0	1.4935 -1.2873	1.3071 -1.3071	0.8537 -1.0848	32.19 -22.39	24.03 -24.03
-10	1.0551 -.9456	1.1610 -.9428	0.5014 -.8694	25.77 -13.53	16.28 -15.22
-20	0.6619 -.6167	0.8108 -.5979	0.2537 -.6154	13.92 -6.90	7.97 -7.99
-30	0.2880 -.2977	0.4290 -.2781	0.0859 -.3203	4.45 -2.34	2.65 -2.74

TABLE II.- POSITION LIMITS OF THE OTHER FIVE DEGREES OF FREEDOM FOR A STATIC POSITION OF THE SIXTH DEGREE OF FREEDOM – Continued

(e) The pitch degree of freedom θ

θ static position, deg	Position limits				
	x, m	y, m	z, m	ψ, deg	ϕ, deg
30	0.2464 -.6373	0.1209 -.1209	0.2162 -.0655	3.78 -3.78	4.98 -4.98
20	0.5466 -1.3561	0.5982 -.5982	0.4483 -.3820	14.69 -14.69	10.96 -10.96
10	0.9119 -1.4224	0.9860 -.9860	0.6645 -.7236	23.46 -23.46	18.38 -18.38
0	1.4935 -1.2873	1.3071 -1.3071	0.8537 -1.0848	38.15 -38.15	24.03 -24.03
-10	1.3713 -1.1600	0.5679 -.5679	0.4757 -.8839	14.91 -14.91	27.25 -27.25
-20	1.1176 -1.0503	0.0861 -.0861	0.0907 -.6756	2.45 -2.45	21.96 -21.96

TABLE II.- POSITION LIMITS OF THE OTHER FIVE DEGREES OF FREEDOM FOR A STATIC POSITION OF THE SIXTH DEGREE OF FREEDOM – Concluded

(f) The roll degree of freedom ϕ

ϕ static position, deg	Position limits				
	x, m	y, m	z, m	ψ, deg	θ, deg
20	0.2398 -.2289	1.2568 -.2235	0.1521 -.4315	4.40 -6.68	8.21 -21.81
10	0.6393 -1.0005	1.2957 -1.1946	0.5192 -.7572	16.95 -17.12	21.50 -22.06
0	1.4935 -1.2873	1.3071 -1.3071	0.8537 -1.0848	38.15 38.15	32.19 -22.39
-10	0.6393 -1.0005	1.1946 -1.2957	0.5192 -.7572	17.12 -16.95	21.50 -22.06
-20	0.2398 -.2289	0.2235 -1.2568	0.1521 -.4315	6.68 -4.40	8.21 -21.81

TABLE III.- NEUTRAL-POINT LOCATION FOR MAXIMUM SYMMETRIC MOTION IN EACH INDIVIDUAL DEGREE OF FREEDOM

Degree of freedom	z_{neut}, m	Position limits					
		x, m	y, m	z, m	ψ, deg	θ, deg	ϕ, deg
x	0.5867	1.3175 -1.3167	1.3371 -1.3371	0.8153 -1.1234	33.99 -33.99	33.48 -21.37	23.02 -23.02
y	0.5725	1.2494 -1.3307	1.3510 -1.3510	0.7971 -1.1417	32.35 -32.35	34.11 -20.89	22.53 -22.53
z	0.7087	1.4651 -1.1930	1.2121 -1.2121	0.9695 -.9695	36.19 -36.19	28.35 -25.49	27.09 -27.09
ψ	0.6233	1.5423 -1.2807	1.3005 -1.3005	0.8621 -1.0767	39.24 -39.24	31.90 -22.61	24.25 -24.25
θ	0.7470	1.4188 -1.1519	1.1707 -1.1707	1.0175 -.9213	34.78 -34.78	26.80 -26.79	28.36 -28.36
ϕ	0.7475	1.4183 -1.1514	1.1702 -1.1702	1.0178 -.9205	34.77 -34.77	26.78 -26.81	28.38 -28.38

TABLE IV.- NEUTRAL-POINT LOCATION FOR MAXIMUM SYMMETRIC HEAVE MOTION WITH A SUSTAINED PITCH ANGLE

θ, deg	z_{neut}, m	z limits, m
6	0.6660	0.8039 -.8037
8	0.6523	0.7496 -.7496
10	0.6401	0.6939 -.6939
12	0.6289	0.6383 -.6380

TABLE V.- WASHOUT PARAMETER VALUES USED IN THE SAMPLE FLIGHT

Variable	Value in SI Units	Program value
$k_{z,1}$	0.8	0.8
$\xi_{z,1}$	0.7	0.7
$\omega_{n,z,1}$, rad/sec	2.0	2.0
$k_{z,2}$	1.0	1.0
$k_{p,T,1}$, per m (per ft)	0.105	0.032
$k_{p,T,2}$, sec	3.8	3.8
$k_{p,T,3}$, per sec	0.01	0.01
$k_{q,T,1}$, per m (per ft)	0.105	0.032
$k_{q,T,2}$, sec	3.8	3.8
$k_{q,T,3}$, per sec	0.01	0.01
$k_{r,1}$, per m (per ft)	0.0131	0.004
$k_{r,2}$, sec	3.8	3.8
$k_{r,3}$, per sec	0.05	0.05
a_1, rad/sec	0.14	0.14
a_2, rad/sec	0.14	0.14
a_3, rad/sec	0.14	0.14
b_1, rad/sec	0.01	0.01
b_2, rad/sec	0.01	0.01
b_3, rad/sec	0.01	0.01
$\ddot{x}_l$, m/sec^2 (ft/sec^2)	5.8840	19.3044
$\ddot{y}_l$, m/sec^2 (ft/sec^2)	5.8840	19.3044
$\ddot{z}_l$, m/sec^2 (ft/sec^2)	7.8453	25.7392
A_1, sec^2	0	0
A_2, sec^2	0	0
A_3, sec^2	0	0

Variable	Value in SI Units	Program value
B_1, sec	0	0
B_2, sec	0	0
B_3, sec	0	0
$k_{\psi,l}$, sec	0	0
$k_{\theta,l}$, sec	0	0
$k_{\phi,l}$, sec	0	0
k_p	0.7	0.7
k_q	0.5	0.5
k_r	0.5	0.5
C_1, per sec	2.0	2.0
C_2, per sec	1.0	1.0
C_3, per sec	2.0	2.0
$k_{\theta,1}$	1.0	1.0
$k_{\theta,2}$	0.04	0.04
ξ_θ	0.028	0.028
$\omega_{n,\theta}$, rad/sec	1.0	1.0
$k_{\phi,1}$	1.0	1.0
$k_{\phi,2}$	0.04	0.04
ξ_ϕ	0.028	0.028
$\omega_{n,\phi}$, rad/sec	1.0	1.0
z_{neut}, m (ft)	0.6487	2.128
V_ℓ, m/sec (ft/sec)	0.3048	1.0
x_{LF}	2.5	2.5
y_{LF}	2.5	2.5
z_{LF}	3.0	3.0

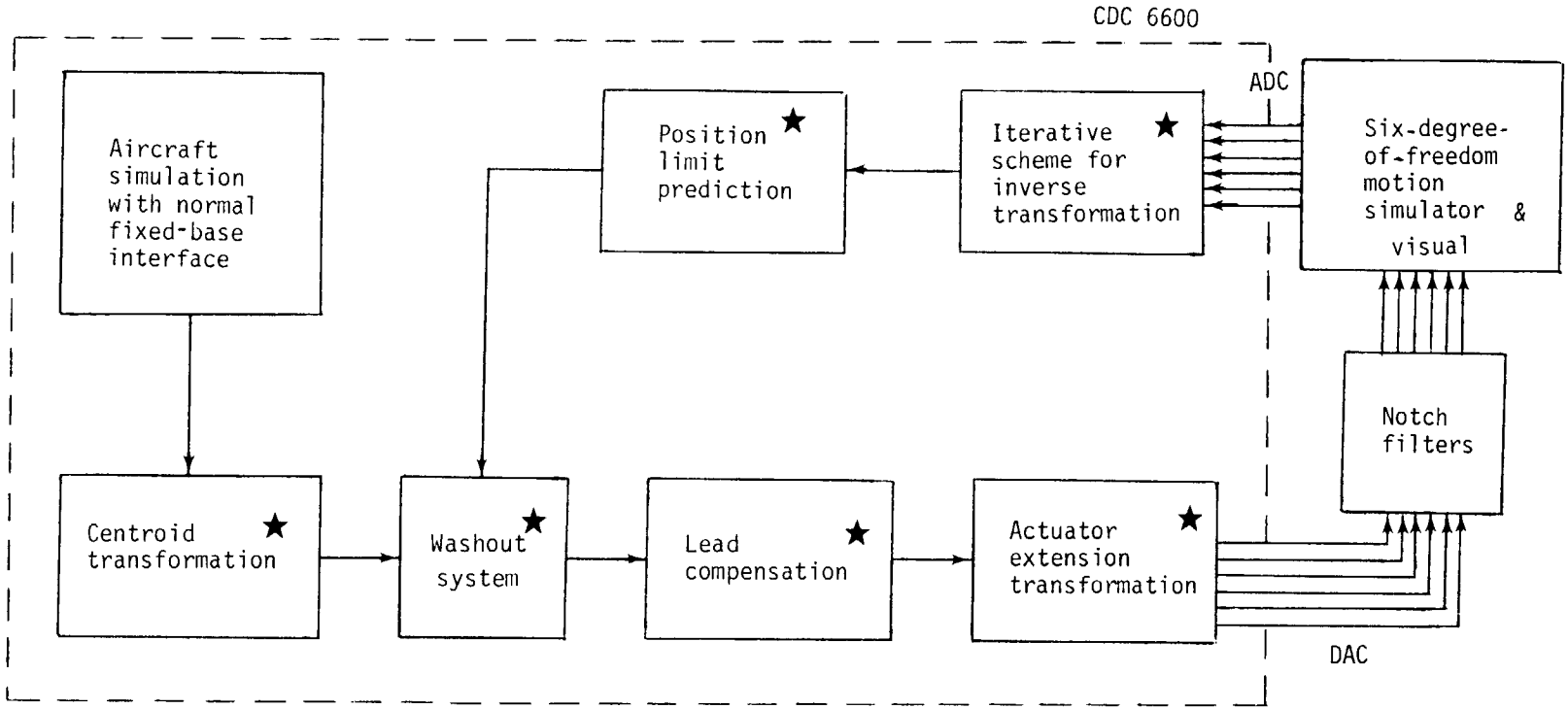

Figure 1.- Major blocks of a real-time motion simulation. Starred blocks indicate the additional software required.

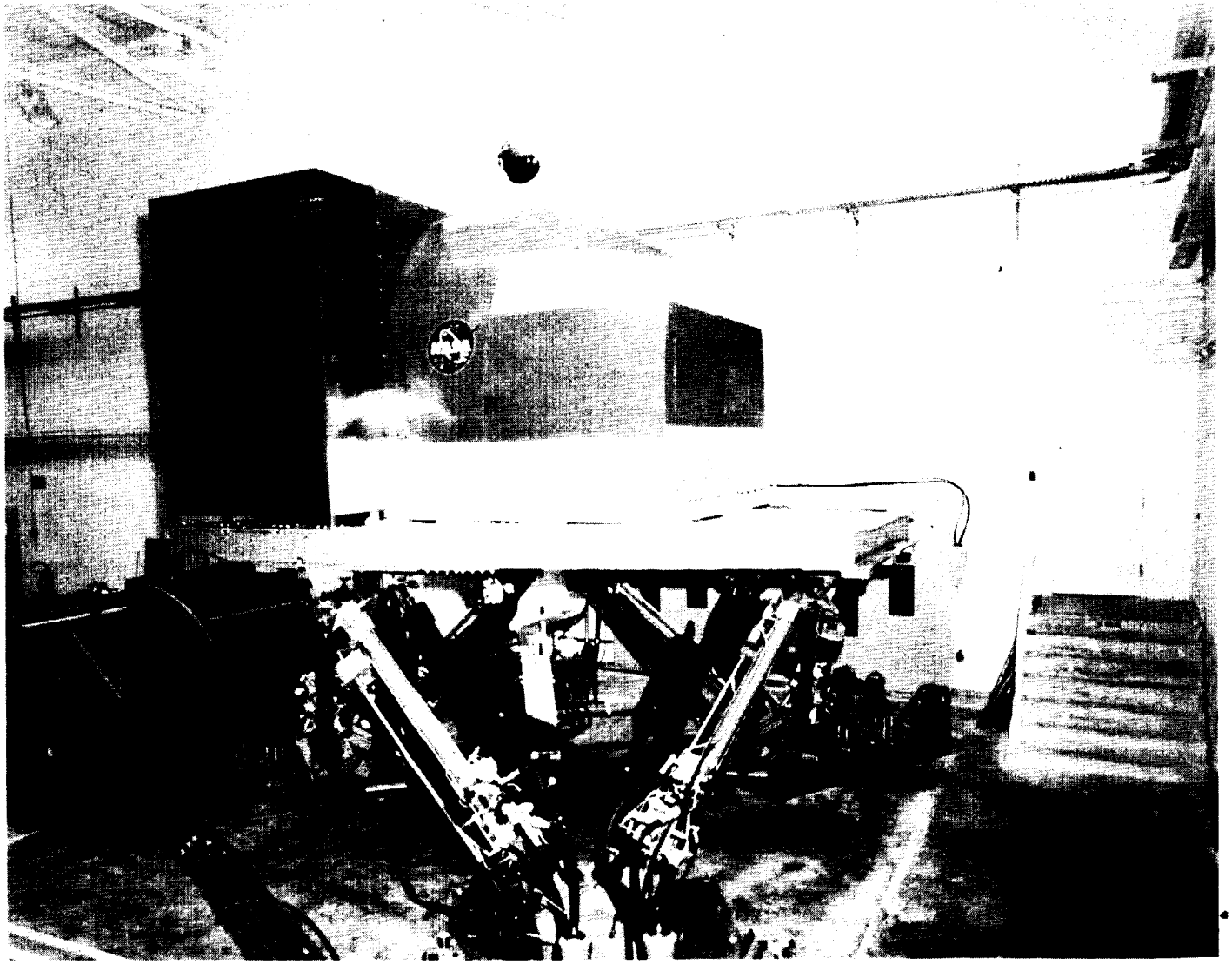

L-72-3233

Figure 2.- Langley six-degree-of-freedom motion simulator.

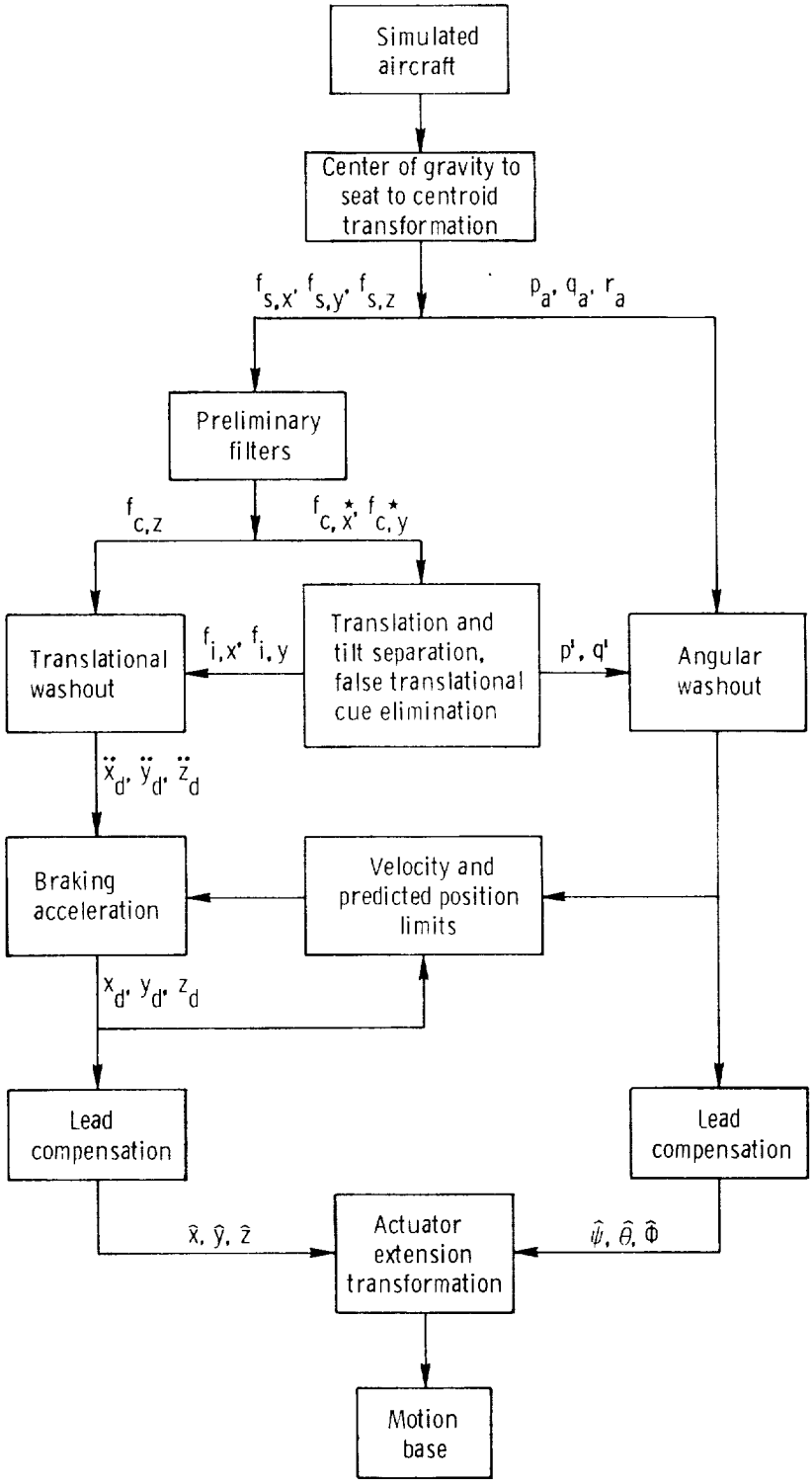

Figure 3.- Block diagram illustrating concept of washout circuitry.

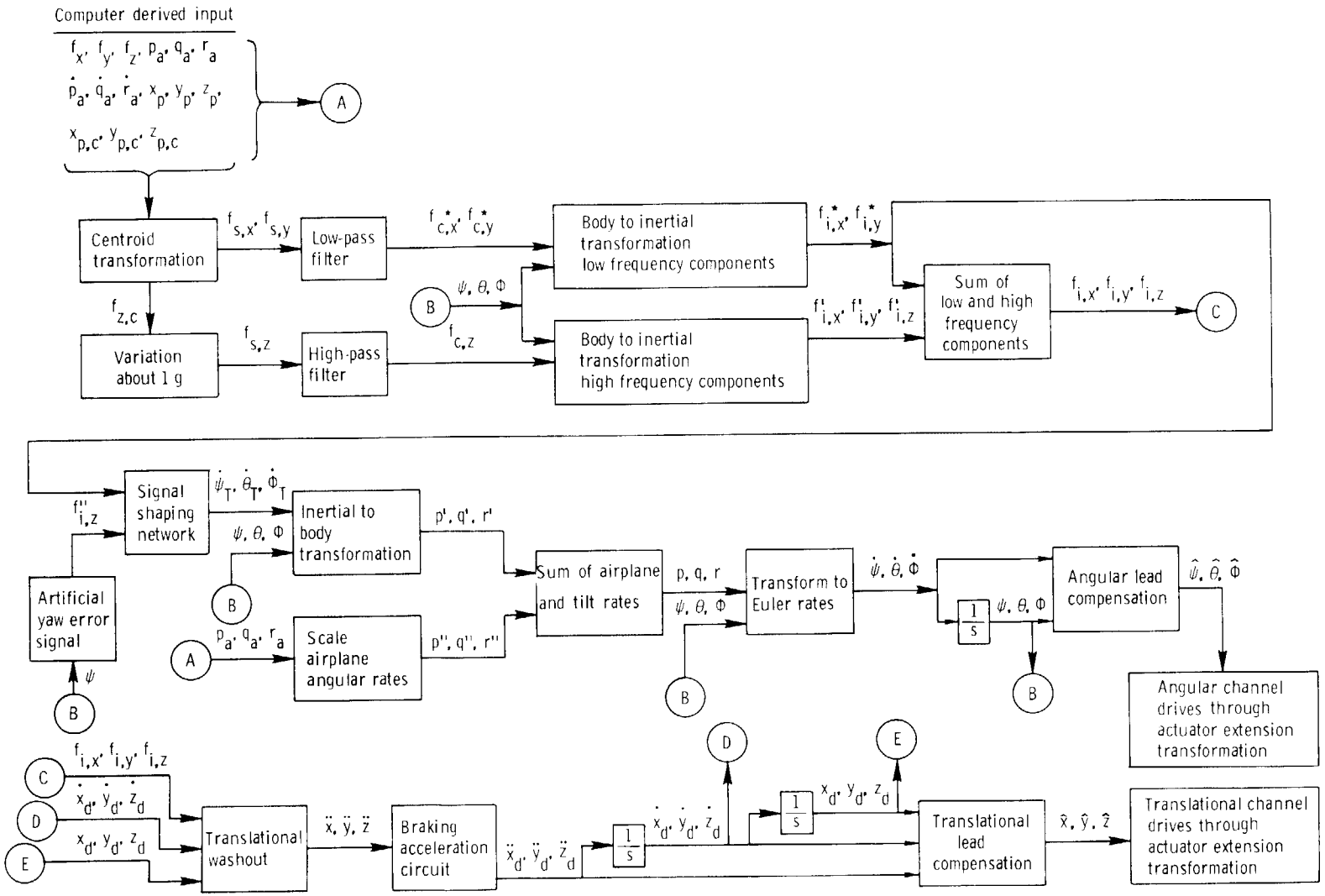

(a) Complete diagram.

Figure 4.- Detailed block diagram of washout circuitry.

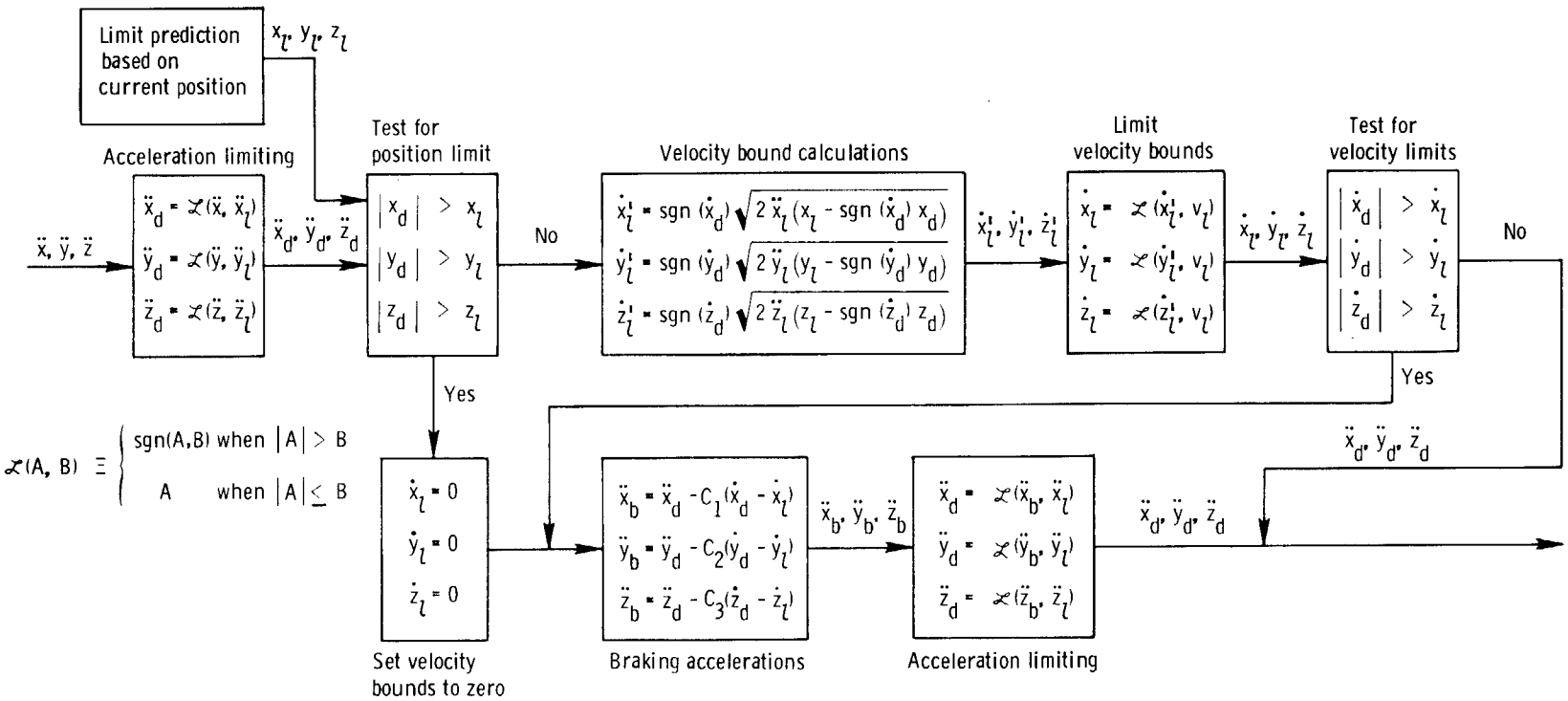

(b) Braking acceleration circuit.

Figure 4.- Concluded.

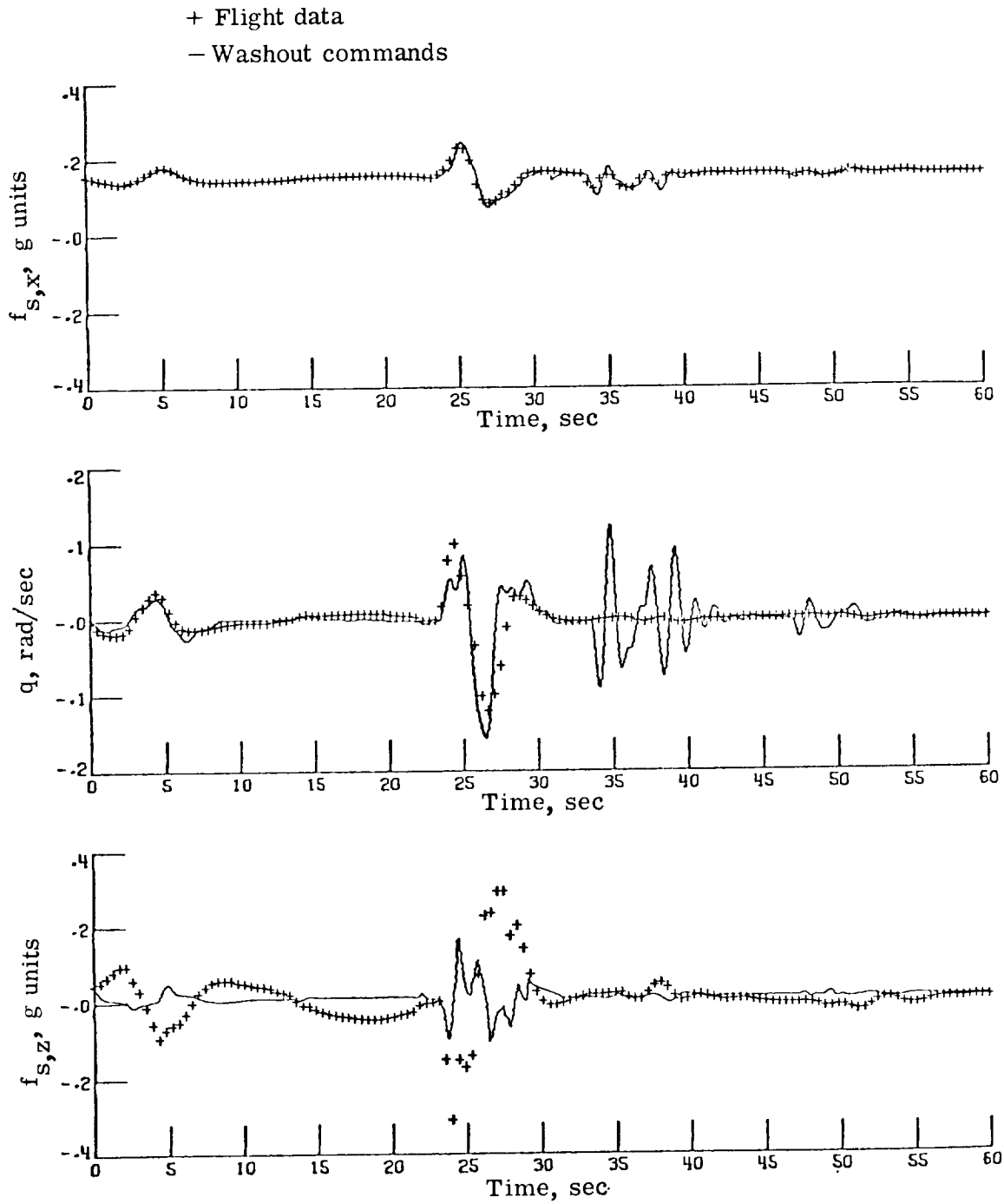

Figure 5.- Comparison of flight data with commanded motion cues.

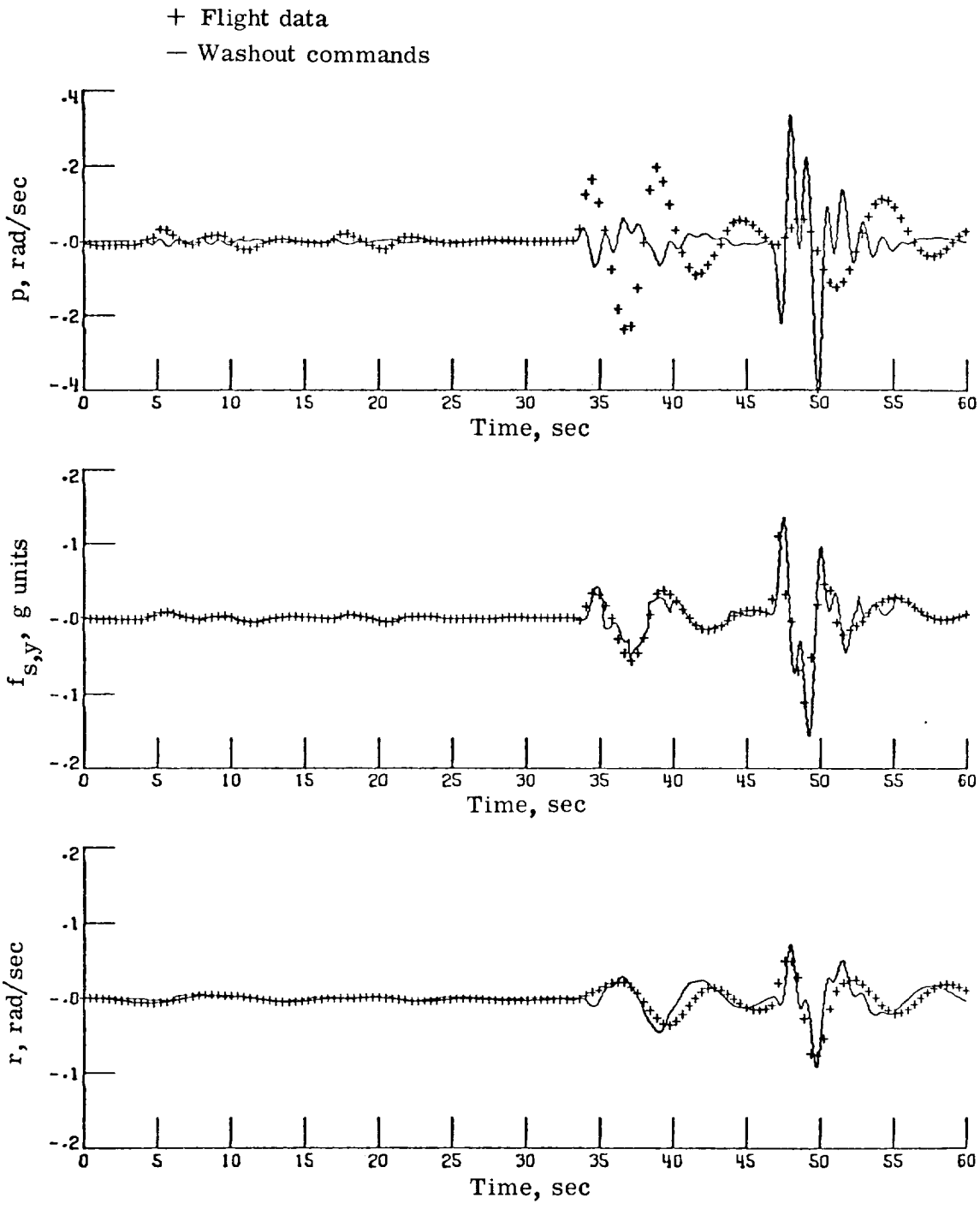

Figure 5.- Concluded.

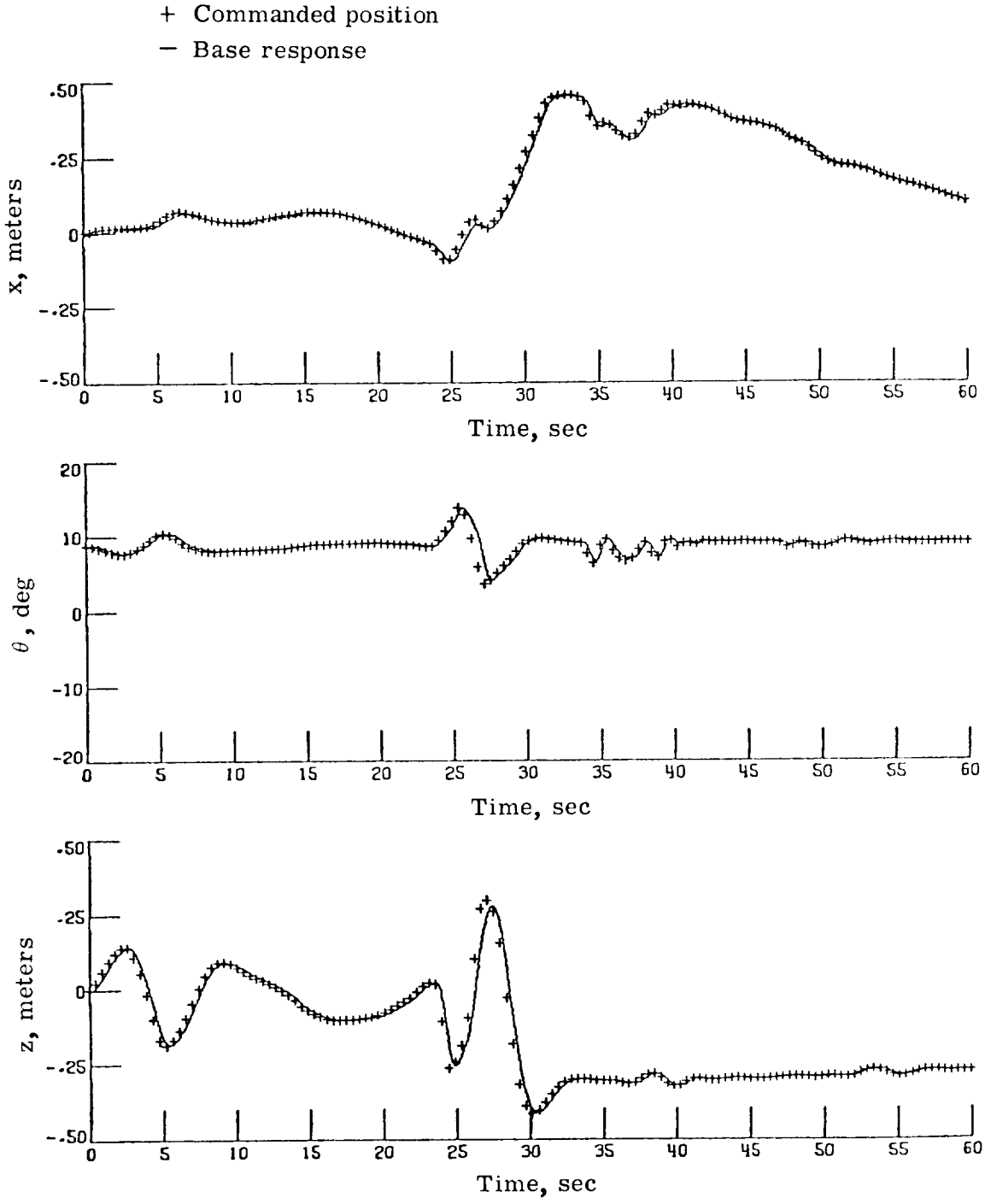

Figure 6.- Comparison of commanded positions and actual base response.

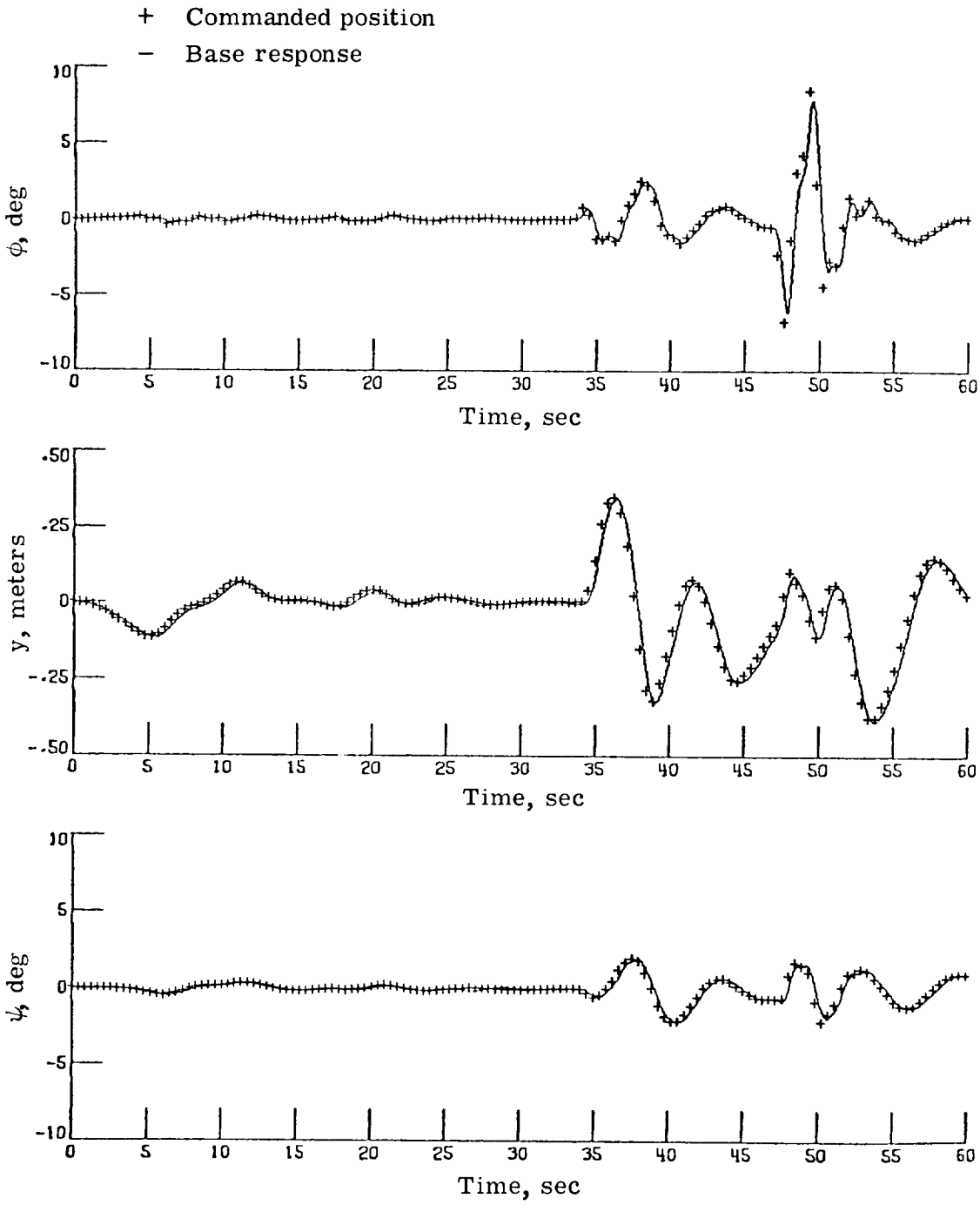

Figure 6.- Concluded.

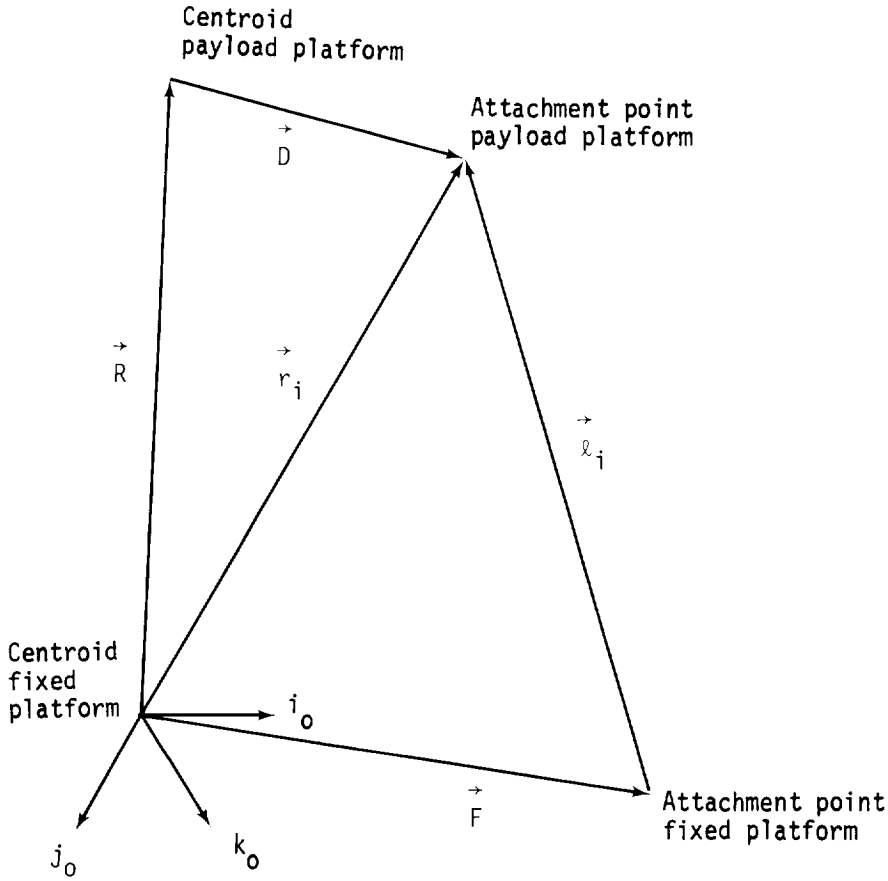

Figure 7.- Vector relationships for actuator i.